Electromechanically driven and sensed parametric resonance in silicon microcantilevers

Michael V. Requa[a] and Kimberly L. Turner
Department of Mechanical and Environmental Engineering, University of California at Santa Barbara, Santa Barbara, California 93106

(Received 22 February 2006; accepted 22 May 2006; published online 26 June 2006)

We report on the design and experimental measurements of an integrated driving and sensing technique in parametrically excited silicon microcantilevers. The design involves actuation with axial Lorentz forces and sensing with magnetomotive forces, both of which are enabled by a chip-scale permanent magnet. In this demonstration the micromechanical parametric resonance is measured electrically. This system has applications to resonant parametric sensing. © *2006 American Institute of Physics*. [DOI: 10.1063/1.2216033]

Cantilevers have long been the standard for resonant micro- and nanoscale force and mass sensors due to their high sensitivities to these influences. The technology of integrating the drive and sense of these transducers is advanced to the point of enabling low-noise feedback controllers.[1,2] Understanding of parametrically excited oscillators, in contrast, is fledgling, due in part to the inherently nonlinear nature of these systems[3] and their recent introduction into the micro- and nanosystems field.[4,5] The technology invested in exploring transducer physics of cantilever systems can also be leveraged to investigate parametrically driven effects. Towards this end we report on a parametrically driven microcantilever transducer design that can be well described by few parameters.

The oscillations of the cantilever can be reduced to a set of second order differential equations by assuming the system to be a collection of linearly independent free-oscillation modes $X(x,t)=\Sigma_{i=0}^{\infty}q_i(t)\varphi_i(x)$. The solution involves simultaneous eigenvalue-eigenfunction of the Euler-Bernoulli beam equation

$$EI\frac{d^4X}{dx^4}+\rho A\frac{d^2X}{dt^2}=0. \qquad (1)$$

The result, for each mode, is a second order differential equation $\ddot{q}+\omega_i^2 q=0$ with one parameter, resonant frequency ω_i. In practice, a description of an oscillator is incomplete without the inclusion of terms to account for damping and deviation from Hooke's linear relationship for large amplitude. For this study a viscous damping term and a cubic stiffness term will suffice. The resulting differential equation for forced oscillation of the primary mode is then

$$\ddot{q}+2\mu\dot{q}+\omega_0^2 q+\gamma q^3=f(t), \qquad (2)$$

where μ, γ, and f are the viscous damping, cubic stiffness nonlinearity, and forcing parameters, respectively, all normalized by the effective modal mass. Consider now a cantilever system that is driven by a force $P(t)$ orthogonal to the spatial coordinate q. The Euler-Bernoulli is modified to

$$EI\frac{d^4X}{dx^4}+P(t)\frac{d^2X}{dx^2}+\rho A\frac{d^2X}{dt^2}=0. \qquad (3)$$

The resulting differential equation that describes the oscillation of the beam has a time periodic parameter which replaces the direct forcing term in Eq. (2).

$$\ddot{q}+2\mu\dot{q}+\omega_0^2 q+\gamma q^3+p(t)gq=0, \qquad (4)$$

where $p(t)=P(t)/\rho A$ and g is a dimensionless parameter related to the mode shape. By averaging the effects of the nonlinearity and damping over one period of oscillation one approximates the steady state amplitude of oscillation

$$a^2=\frac{2}{3\gamma}\{4\omega_0\sigma\pm[\lambda^2-(4\omega_0\mu)^2]^{1/2}\}, \qquad (5)$$

where $\sigma=\frac{1}{2}\omega-\omega_0$ and $p(t)=\lambda\cos\omega t$. The resonant frequency is very close to half the driving frequency. For this system to have real, nonzero solutions the driving strength λ must overcome a threshold determined by the damping and resonant frequency

$$\lambda\geqslant 4\omega_0\mu. \qquad (6)$$

By the same method of averaging, one finds the steady state amplitude solutions to a Duffing-type oscillator with a harmonic driving term, Eq. (2). A description of the method of averaging, solutions to the above differential equations [(2) and (4)], and a kinematic derivation of the physical cantilever system can be found in Ref. 6. Figure 1 shows a comparison of the spectral response of the two systems, direct excitation and parametric excitation, having identical parameter value (Table I).

The spectral response of the parametrically excited system has two bifurcation points.[3] If an oscillator is initialized in the zero amplitude attractor and the system is tuned across the leftmost bifurcation point, the amplitude will jump up to the high amplitude solution which is then the only stable state. The presence of this bistable region and the corresponding bifurcation to a single solution state offers a dramatic "jump" transition from a near-zero solution to one of high amplitude. This transition has been explored as a sensing mechanism because it is an indicator of the resonant frequency of the device.[7]

Cantilevers were fabricated from silicon-on-ion-implanted-oxide (SIMOX) wafers with a device layer of

[a]Electronic mail: requa@engr.ucsb.edu

 © 2006 American Institute of Physics
Downloaded 26 Jun 2006 to 128.111.144.42. Redistribution subject to AIP license or copyright, see http://apl.aip.org/apl/copyright.jsp

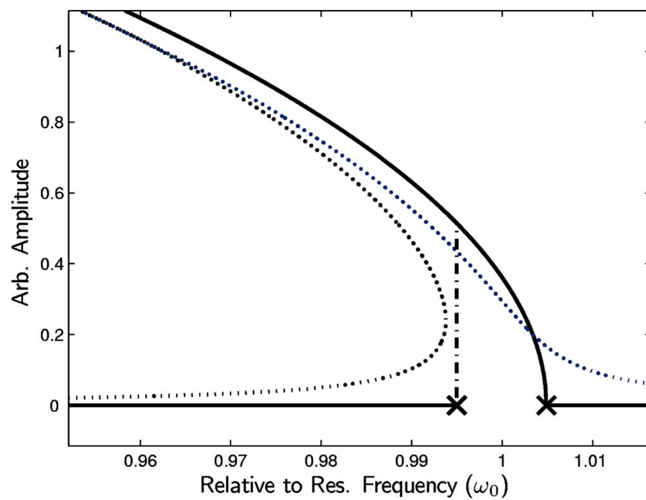

FIG. 1. (Color online) Comparison of Duffing-type oscillator driven with direct forcing (dash) and parametric (solid). Represents resonators with identical parameters (see below). Vertical line represents "jump" phenomenon at the bifurcation point indicated by x. For this analysis, cubic nonlinearity is negative.

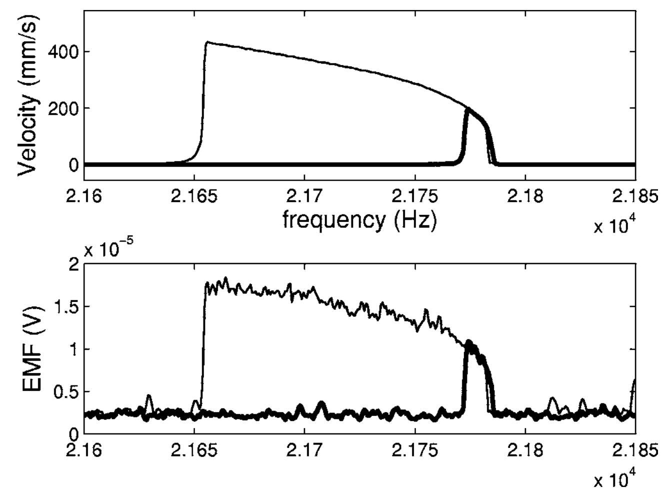

FIG. 2. Simultaneously measured system response. Top is from laser vibrometer bottom is measured emf. Demonstrated is the hysteresis predicted by theory. Heavy is sweep up in frequency, light is sweep down.

200 nm. Fabricating oscillators from this material system has been previously characterized[8] and extended to be used as highly sensitive resonant mass sensors.[9] For this reason we omit most process details. A backside through wafer dry etch was performed to remove the Si handle material below the oscillator using a SF_6 plasma and the buried oxide layer as an etch stop. A blanket layer of evaporated metal 20 nm thick (10 nm Ti/10 nm Au) was deposited using electron beam evaporation to enhance conductivity. The layer of metal reduced the Q factor of the resonators to 1000 under vacuum. Quality factor and resonant frequency were measured using a piezoelectric crystal to harmonically excite the cantilever with a frequency sweep near its resonant frequency and a laser Doppler vibrometer to measure the response. Relationship (6) indicates that the force required to generate parametric resonance is proportional to the damping coefficient and resonant frequency. In the present demonstration this requires using ultrathin cantilevers operated in vacuum. The force is limited by the electrical capacity of the metal layer.

Data are presented for a device which is 60 μm long, with all lateral features being 5 μm wide and a thickness of 200 nm. The measured resonant frequency is near 21.75 kHz (Fig. 2). The cantilever is oriented in the magnetic field in such a way that there are significant components of the field both parallel (x direction) and orthogonal (z direction) to the long axis of the cantilever. These components provide the field for inducing parametric driving and sensing, respectively (Fig. 3).

We employ a U-shaped cantilever to realize a parametric axial load. An alternating current is applied through the cantilever which, by Lorentz interaction, generates a force $P(t)$ in the end member which is parallel to the long axis of the cantilever (x direction). It is this force that parametrically drives the out of plane oscillation. The end of the cantilever oscillates perpendicularly to the sensing field generating an electromotive force which can be measured to observe the oscillation. The driving signal amplitude is at twice the frequency of the sensing signal which makes the sensing signal measurable against a driving signal that is several orders larger. In this case the driving source is current controlled to be 5×10^{-4} A. The device impedance is measured to be 400 Ω resulting in a drive signal of 200 mV at near 43.5 kHz. The same terminal of the device is then connected to the input channel of a low pass filter set with a cutoff frequency intermediate to drive and sense. The signals exist on the same electrodes which accommodates further device miniaturization as the device size approaches minimum feature size and having two isolated conductors becomes implausible. The output of the low pass filter is connected to a spectrum analyzer to read the frequency swept signal. In parallel to this electronic measurement a laser Doppler vibrometer system makes a simultaneous and independent measurement of velocity. The vibrometer signal is read by the same spectrum analyzer. The emf measured is on the order of 10 μV, four orders smaller than the driving signal.

Several past experiments demonstrating similar magnetomotive forcing mechanisms have been performed using supercooled electromagnets capable of generating fields as

TABLE I. Parameter values for spectral comparison as plotted in Fig. 1.

ω_0	μ	γ	f (harmonic)	λ (parametric)
1	0.001	−0.001	0.02	0.02

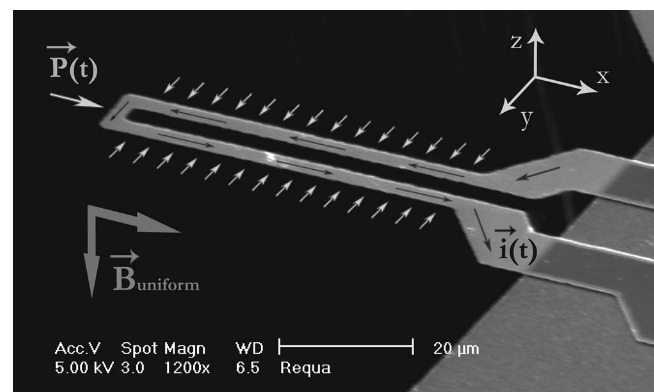

FIG. 3. SEM of U-shaped cantilever with superimposed forces, currents, and fields. The chip is placed on top of a permanent magnet (NdFeB) during operation. Magnetic field strength is near 1 T.

Downloaded 26 Jun 2006 to 128.111.144.42. Redistribution subject to AIP license or copyright, see http://apl.aip.org/apl/copyright.jsp

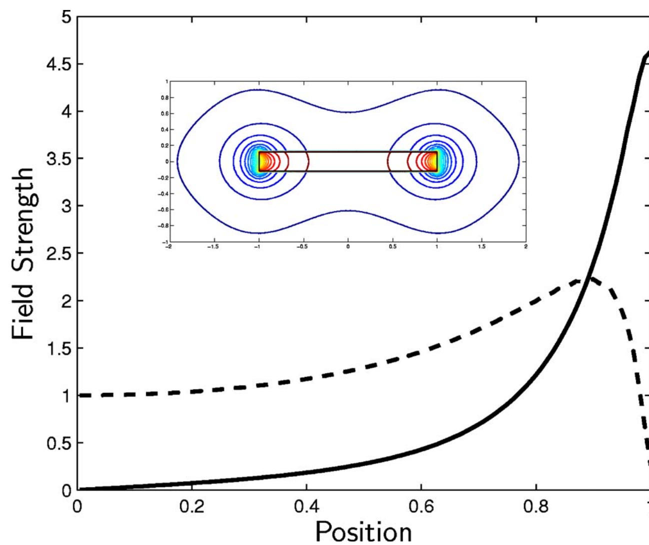

FIG. 4. (Color online) Magnitude of magnetic field for driving (dash) and sensing (solid) fields at a distance of the chip thickness from the surface of the magnet, values correspond roughly to teslas. Optimal operation location is at maximum of two fields. (Inset) FE simulation of magnetic field lines for magnet similar in aspect ratio to that used in experiment.

high as an 8 T with controlled orientation.[10] This work employs a NdFeB permanent magnet with dimensions of $25 \times 12 \times 3$ mm^3. The device chip, comparable in size, rests on the largest face of the magnet during experiment. Some control in the field strength and orientation can be gained by using the field concentrations near the edges of the magnet. A finite element simulation of magnetic field lines was performed to find the ideal operating position of the resonator in relationship to the magnet in order to maximize both essential field components. A cross section of this simulated field taken at a distance equal to the wafer thickness from the surface is represented in Fig. 4 and shows the optimal operating point to be approximately 89% to the edge from the magnet center. At this, the ideal point, the signal strength to achieve parametric excitation by Eq. (4) is minimized, while the emf induced approaches a maximum.

Sensors designed to exploit parametric amplification are still in their infancy. Several characteristics make them promising. The hysteresis and jump phenomenon persist so long as the driving term is above a critical threshold, while the theoretical sensitivity of a harmonic oscillator decays with damping.[11] The jump phenomenon is so dramatic that it may be more easily measured over an electronic noise floor. Cantilevers have been fundamental in forwarding harmonic resonant sensing and may prove so for parametric excited sensing as well. This work makes a demonstration of an integrated electromechanical drive and readout of a parametrically excited microsystem, but further makes a cantilever platform for parametric resonance which can be described by a minimal number of parameters.

[1]E. Forsen, G. Abadal, S. Ghatnekar-Nilsson, J. Teva, J. Verd, R. Sandberg, W. Svendsen, F. Perez-Murano, J. Esteve, E. Figueras, F. Camapabadal, L. Montelius, N. Barniol, and A. Boisen, Appl. Phys. Lett. **87**, 043507 (2005).
[2]D. Lange, Ph.D. thesis, ETH Zurich, 2000.
[3]M. I. Dykman, C. M. Maloney, V. N. Smelyanskiy, and M. Silverstein, Phys. Rev. E **57**, 5202 (1998).
[4]K. L. Turner, S. A. Miller, P. Hartwell, N. C. MacDonald, S. H. Strogatz, and S. G. Adams, Nature (London) **396**, 149 (1998).
[5]M. Zalalutdinov, A. Olkhovets, A. Zehner, B. Ilic, D. Czaplewski, and H. G. Craighead, Appl. Phys. Lett. **78**, 3142 (2001).
[6]A. H. Nayfeh and D. T. Mook, *Nonlinear Oscillations* (Wiley, New York, 1977).
[7]W. Zhang and K. L. Turner, Proceedings of 2004 ASME International Mechanical Engineering Congress (ASME, Anaheim, CA, 2004).
[8]J. Yang, T. Ono, and M. Esashi, Sens. Actuators, A **A82**, 102 (2000).
[9]B. Ilic, H. G. Craighead, S. Krylov, W. Senaratne, C. Obera, and P. Nuezil, J. Appl. Phys. **95**, 3694 (2004).
[10]A. N. Cleland and M. L. Roukes, Appl. Phys. Lett. **69**, 2653 (1996).
[11]T. R. Albrecht, P. Grütter, D. Horne, and D. Rugar, J. Appl. Phys. **69**, 668 (1991).

Downloaded 26 Jun 2006 to 128.111.144.42. Redistribution subject to AIP license or copyright, see http://apl.aip.org/apl/copyright.jsp